

Electronic Supplementary Information
Towards a traceable enhancement factor in surface-enhanced Raman spectroscopy

Eleonora Cara,^{*a} Luisa Mandrile,^a Alessio Sacco,^a Andrea M. Giovannozzi,^a Andrea M. Rossi,^a Federica Celegato,^a Natascia De Leo,^a Philipp Hönicke,^b Yves Kayser,^b Burkhard Beckhoff,^b Davide Marchi,^c Alberto Zoccante,^c Maurizio Cossi,^c Michele Laus,^c Luca Boarino^a and Federico Ferrarese Lupi^a

^a Istituto Nazionale di Ricerca Metrologica (INRiM), Strada delle Cacce 91, 10135 Torino, Italy. *E-mail: e.cara@inrim.it

^b Physikalisch-Technische Bundesanstalt (PTB), Abbestr. 2-12, 10587 Berlin, Germany.

^c Dipartimento di Scienze e Innovazione Tecnologica, Università del Piemonte Orientale (UPO), Via T. Michel 11, 15100 Alessandria, Italy

1 Evaluation of the scattering volume

The determination of the scattering volume was carried out experimentally by means of the methodology reported in references 1–3. The parameters affecting the uncertainty on this measurement are related to the sensitivity of the microscope stage motors in each direction. The relative uncertainty on the confocal volume was estimated to be approximately 5 %. In Figure S1, the intensity profile of the Raman microscope employed in this work is shown as a function of the displacement along the depth direction. The confocal volume was modelled as an ellipsoid with the two minor axes equal to the laser spot diameter. The major axis was estimated by considering the z position corresponding to a decrease to $1/e^2$ of the maximum intensity of the least-squares Gaussian regression on the data (approximately 13.5 %, corresponding to a total range of 4 times the width parameter of the Gaussian curve). The long axis of the ellipsoid was measured to be $(62 \pm 2) \mu\text{m}$. The uncertainties on the dimensional data on the confocal volume are given by the sensitivity of the piezoelectric motors in the Raman microscope stage. The total laser-probe interaction volume was calculated to be $V = (364 \pm 20) \mu\text{m}^3$.

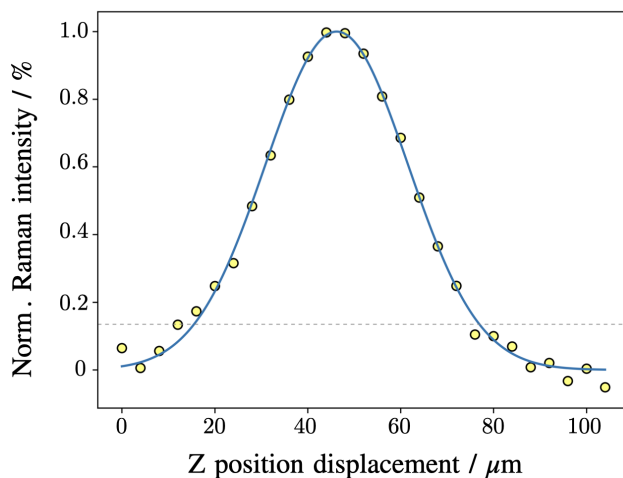


Figure S1 Scatter plot of the intensity of the profile of the Raman microscope normalised to the intensity at the focal plane as a function of the displacement along the depth direction axis, with superimposed Gaussian curve best fit (solid blue) employed to calculate the confocal depth and intensity threshold used for the definition of the volume (dashed grey).

2 Geometrical considerations on the molecular surface density

The value of $\mu_{\text{MMC/geom}}$ derived from model 1 carries an uncertainty propagated from the one associated with the molar volume. The values of $\mu_{\text{MMC/geom}}$ for models 2 to 4 do not have an associated uncertainty. The contribution to the uncertainty for $N_{\text{SERS/geom}}$ corresponding to the different models was propagated from the total surface area inside the scattering volume and it is equal to 21.8 %. The graphical schemes for the derivation of $\mu_{\text{MMC/geom1}}$ and $\mu_{\text{MMC/geom2}}$ are reported in Figure S2a and b, respectively.

The monolayer density on a perfectly flat surface was determined on a geometrical basis for $\mu_{\text{MMC/geom3}}$ and $\mu_{\text{MMC/geom4}}$, assuming an Au-Au distance of 2.77 Å (as derived from the crystalline structure) and the following covalent radii in angstrom: H 0.3; C 0.6; O 0.6; S 1.0. As shown also by the MM optimizations presented in the text, while the concentration of adsorbed molecules is very low, each MMC tends to lie down on the surface to maximize the host-guest interactions, but as the monolayer becomes dense, the molecules stand up, maximizing the lateral guest-guest interactions. There are two possible conformations for the MMC units in a dense, ordered monolayer, i.e. “vertical” or “lateral” arrangement, as shown in Figure S3a-b. Using the atomic sizes listed above, the minimum distance between adjacent molecules were determined in both arrangements, obtaining the densest monolayers which can be formed on the flat surface, as illustrated in Figure S3c-d. The corresponding molecular densities are $\mu_{\text{MMC/geom3}} = 3.6 \text{ nm}^{-2}$ for the lateral and $\mu_{\text{MMC/geom4}} = 5.0 \text{ nm}^{-2}$ for the vertical arrangement.

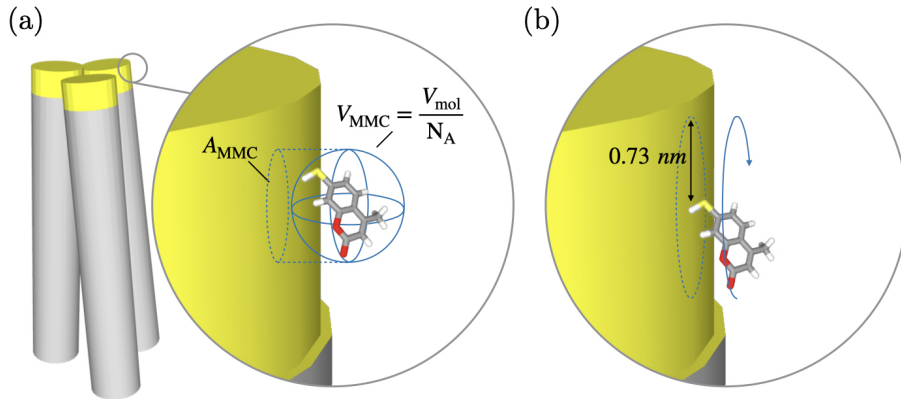


Figure S2 Schematic representation (in exaggerated scale) of the starting assumptions for the geometrical calculation of (a) $\mu_{\text{MMC/geom}1}$ through the molar volume to determine the occupancy of a spherical molecule and (b) of $\mu_{\text{MMC/geom}2}$ through a molecule rotating around the thiol group.

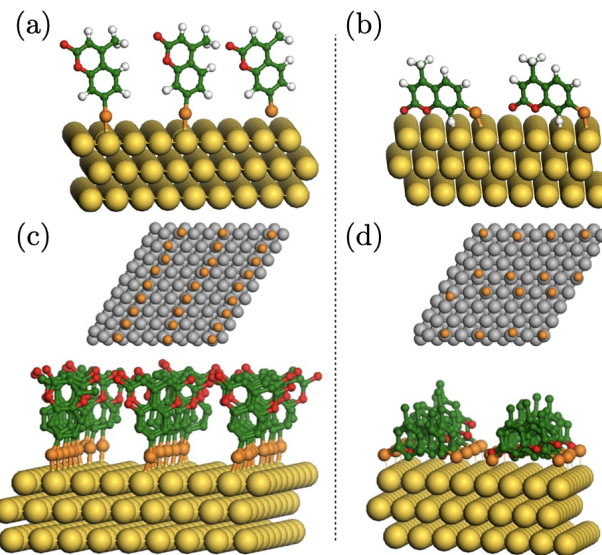


Figure S3 MMC molecules attached to the gold surface in the (a) vertical or (b) lateral arrangement. Corresponding monolayer structure for the (c) vertical and (d) lateral conformations. Hydrogen atoms not shown for clarity.

3 Determination of the force field (FF) for MM and MD simulations.

To model the molecular monolayers of 7-mercaptop-4-methylcoumarin (MMC) on gold (111) surfaces, the most relevant contributions come from MMC/MMC interactions and MMC/Au interactions, while a limited weight is expected for the intramolecular bond parameters. We started from the universal force field (UFF) which provides parameters for all the relevant bond lengths and angles, except S-Au, and for the non-bonded interactions through Lennard-Jones dispersion/repulsion curves. The FF reliability was checked against DFT calculations on model systems, using B3LYP hybrid functional, Dunning's correlation consistent cc-PVDZ basis set for all the light atoms, and Hay-Wadt pseudopotentials and basis sets for S, Au. The dispersion contributions were corrected with the procedure and the parameters proposed by S. Grimme et al⁴. The ab initio calculations have been performed with Gaussian16 suite, and the FF-based classical simulations with LAMMPS. Whenever necessary, basis set superposition error (BSSE)⁵ has been accounted for with the counterpoise method as implemented in Gaussian16. The intermolecular interactions were checked first. As shown in Figure S4, a rigid scan of a MMC dimer was performed varying the distance of the two molecules, computing the DFT energies at all the distances. The ab initio relative energies, referred to the minimum, are reported along with the corresponding relative energies computed by LAMMPS with UFF parameters: the good agreement between the two energy curves indicates the FF is suitable to describe intermolecular lateral interactions.

To describe MMC/surface interactions, we resorted to a small model of the gold surface, extracting an atomic cluster from the (111) surface described in the main text. The cluster comprised two layers with 26 and 20 gold atoms, respectively, and its geometry was kept frozen in all the calculations. One MMC was optimized close to the cluster upper face, and then a rigid scan was performed varying the distance of the molecule from the surface. Since in our model the molecule loses the thiol hydrogen to form a covalent S-Au bond, both the MMC fragment and the cluster are radicals (in doublet spin state when treated separately for the correction of the BSSE). The dispersion-repulsion parameters involving MMC and gold atoms were fitted to this energy scan. Two kinds of S-Au interactions were defined, both described by means of Lennard-Jones (LJ) curves. One refers to the covalent bond and involves only one S-Au couple,

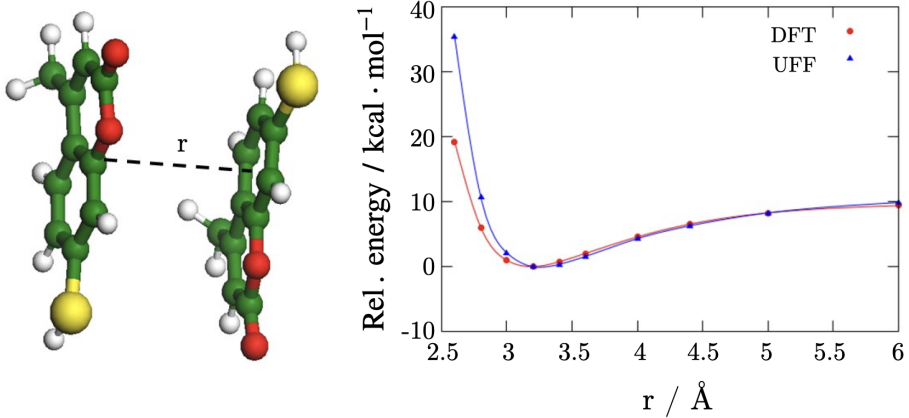


Figure S4 Rigid scan of the MMC/MMC distance, and comparison of ab initio and UFF energies.

Table S1 Lennard-Jones parameters for the MMC/Au interactions fitted to DFT calculations.

Pair	ϵ [kcal/mol]	σ [Å]
C - Au	0.050	3.172
O - Au	0.050	3.024
S - Au (bonded)	24.50	2.495
S - Au (non bonded)	4.203	3.247

the other to non-bonded interactions between sulfur and all the remaining gold atoms. Note that in the former case the LJ parameters designed to reproduce the chemical bond produce a curve markedly deeper and more attractive than the usual dispersion/repulsion curves. We chose this functional form, instead of the harmonic functions commonly used for bond stretching, to allow some MMC to leave the surface if this lowers the system energy, to determine the best monolayer density. All the LJ parameters were fitted to the ab initio scan, with the results shown in Figure S5 and listed in Table S1. The simulated value of the molecular surface density $\mu_{\text{MMC}/\text{simul}}$, derived from deterministic simulation, does not carry an uncertainty. The contribution to the uncertainty for $N_{\text{SERS}/\text{simul}}$, as well as for the geometrical models, was propagated from the total surface area inside the scattering volume and it is equal to 21.8 %.

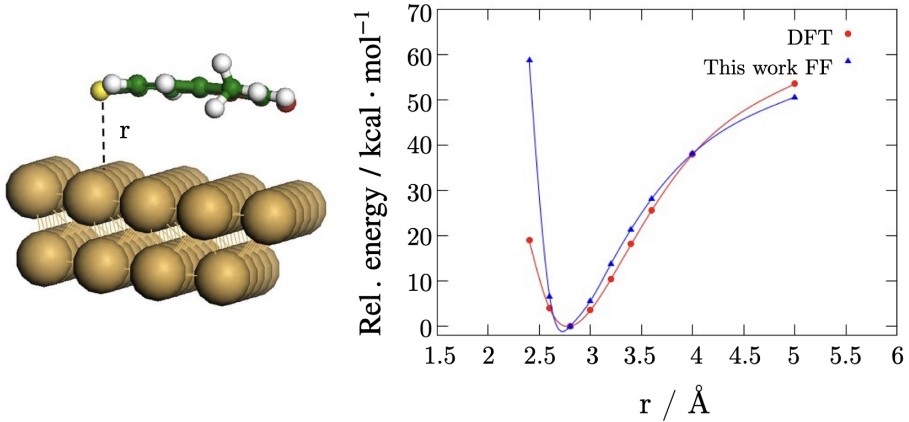


Figure S5 Rigid scan of MMC/gold cluster distance, and results of the FF fitting.

4 Reference-free X-ray fluorescence experiment

The reference-free X-ray fluorescence measurements were conducted using the experimental setup reported in Figure S6. Equation (3) was used for the calculation of the mass of sulfur per unit area on the measured substrates. The uncertainties associated with the measurements were calculated through the standard propagation of uncertainties from the major components. A relative uncertainty of 10 % was considered on the fluorescence yield $\omega_{\text{S,K}}$, and 5 % uncertainty due to the spectral deconvolution⁶. Other smaller contributions to the total uncertainty comprised 4 % on the calculation of the effective solid angle, 3 % relative standard deviation on the calculation of the average of the photon counts $P_{\text{S,K}}$, 2.5 % from the S-K photon counts, and 2 % instrumental uncertainty. The computation of the relative uncertainty produced a value of 12.7 %, this propagated to the total uncertainty on σ_{S} of 15.8 %. The same uncertainty was estimated for $\mu_{\text{MMC/XRF}}$ in which the Avogadro constant, fixed exactly to the value of $6.02214076 \cdot 10^{23} \text{ mol}^{-1}$ in 2018 CODATA, and the atomic weight of sulfur, selected from IUPAC reference value⁷, did not contribute to the uncertainty. The same

standard propagation was applied to the calculation of the uncertainty on the number $N_{\text{SERS/XRF}}$ given by the contribution from the surface density of MMC and the surface area, for a total of 26.9 %.

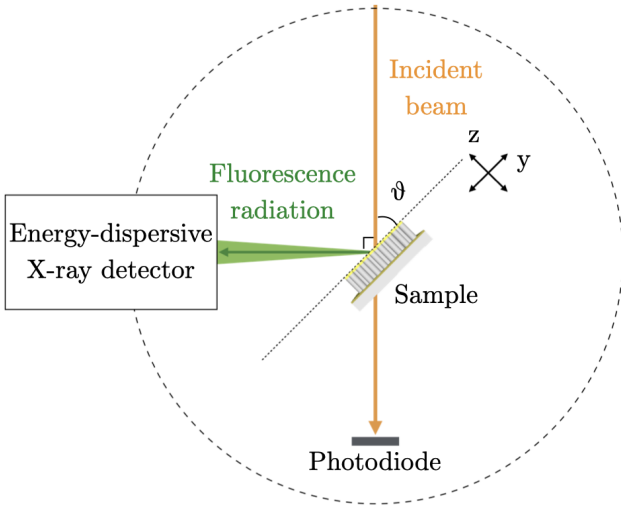


Figure S6 Instrumental setup for the RF-XRF measurements at the PTB beamline at BESSY II electron storage ring.

5 Determination of the enhancement factor

In the evaluation of the enhancement factor with the formula in Equation (1), the single contributions to the uncertainty budget are given by 5 % on the intensity of SERS and normal Raman signals, due to instrumental sensitivity, 10 % on I_{SERS} accounting for the variability among different repetitions, and 5.7 % on the number N_{NR} . The latter is given by combining the uncertainty on the solution concentration, the precision of 0.1 mg of the balance used for the gravimetric preparation of the solution and the volumetric glassware tolerance of 0.1 ml. These three components were further combined with the uncertainty on the scattering volume, which is predominant with respect to other sources of uncertainty for N_{NR} . The standard propagation of the uncertainties for independent variables was applied for the calculation of the total relative uncertainty associated with the EF.

6 Uncertainty evaluation for the metallic surface area

The metallic surface area A_M was measured by means of atomic force microscopy on single nanowires, which were dispersed on a solid substrate by scraping them off the standing nanowires matrix with a semi-rigid thread. The estimation provided by atomic force microscopy presents some intrinsic limitations related to the interaction between the probe tip and corrugated gold surface. Besides, the AFM tip only interacts properly with the upper portion of the horizontal nanowires, approximately one-third of the lateral area of the cylinder, due to the curved surface of the nanowire as shown in Figure S7. The remaining not-scanned two thirds were assumed to have equal surface area so that the total value around the structure was extrapolated. The gold surface area on the top face was measured on isolated gold caps detached from the silicon nanowires during the transfer process of the nanowires. The top and lateral surface area together constitute A_M .

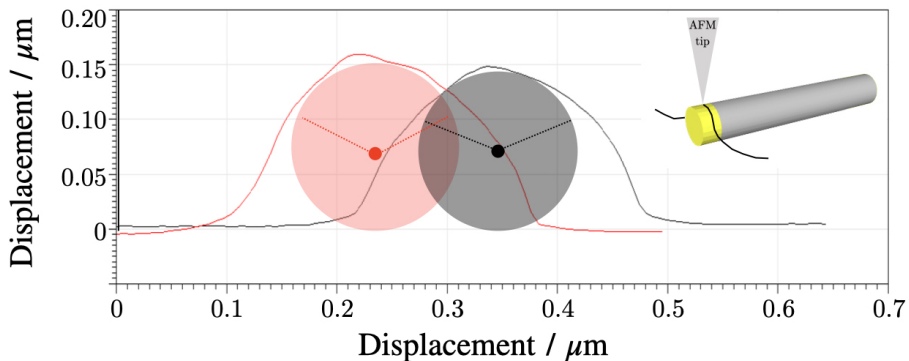


Figure S7 AFM height profile of the nanowires and schematic representation of the measurement in the top right corner. The nanowires sections are depicted to highlight that the top one third of the nanowire is properly scanned by the tip.

The relative uncertainty associated with the displacement of the AFM tip on the XY plane and Z-axis was estimated to be 6.9 % by means of a calibrated standard supplied with the AFM. Employing Gwyddion computation by triangulation, the uncertainty associated

with a single surface area measurement was estimated to be 15.4 %. This value was propagated through different measurements on the SERS tip surface area leading to $A_M = (0.52 \pm 0.09) \mu\text{m}^2$ with a relative uncertainty of 18.3 %.

Notes and references

- [1] Y. Kim, E. J. Lee, S. Roy, A. S. Sharbirin, L.-G. Ranz, T. Dieing and J. Kim, *Current Applied Physics*, 2020, **20**, 71–77.
- [2] C. Korzeniewski, J. P. Kitt, S. Bukola, S. E. Creager, S. D. Minteer and J. M. Harris, *Analytical chemistry*, 2018, **91**, 1049–1055.
- [3] A. D'Agostino, A. M. Giovannozzi, L. Mandrile, A. Sacco, A. M. Rossi and A. Taglietti, *Talanta*, 2020, 120936.
- [4] S. Grimme, J. Antony, S. Ehrlich and H. Krieg, *The Journal of chemical physics*, 2010, **132**, 154104.
- [5] S. F. Boys and F. Bernardi, *Molecular Physics*, 1970, **19**, 553–566.
- [6] M. Müller, P. Hönicke, B. Detlefs and C. Fleischmann, *Materials*, 2014, **7**, 3147–3159.
- [7] M. E. Wieser, N. Holden, T. B. Coplen, J. K. Böhlke, M. Berglund, W. A. Brand, P. De Bièvre, M. Gröning, R. D. Loss, J. Meija *et al.*, *Pure and Applied Chemistry*, 2013, **85**, 1047–1078.